Electronic Supplementary Material (ESI) for Dalton Transactions.

Supporting Information

Monochromatic light-enhanced photocatalytic CO_2 reduction based on exciton properties of two-dimensional lead halide perovskites

Shengqi Xu,[a] Lu Yang,[a] Yixuan Wei,[a] Yiming Jia,[a] Meiqi Hu,[a] Lianxia Bai,[b] Junzheng Zhang,[b] Xinxin Li,[c] Shuo Wei*[a] and Jun Lu[b]

[a.] College of Chemistry, Beijing Normal University, Beijing 100875, P. R. China.

[b.] State Key Laboratory of Chemical Resource Engineering, Beijing University of Chemical Technology, Beijing 100029, P. R. China.

[c.] Analytic and Testing Center, Beijing Normal University, Beijing 100875, P. R. China.

*corresponding author: vshuo@bnu.edu.cn.

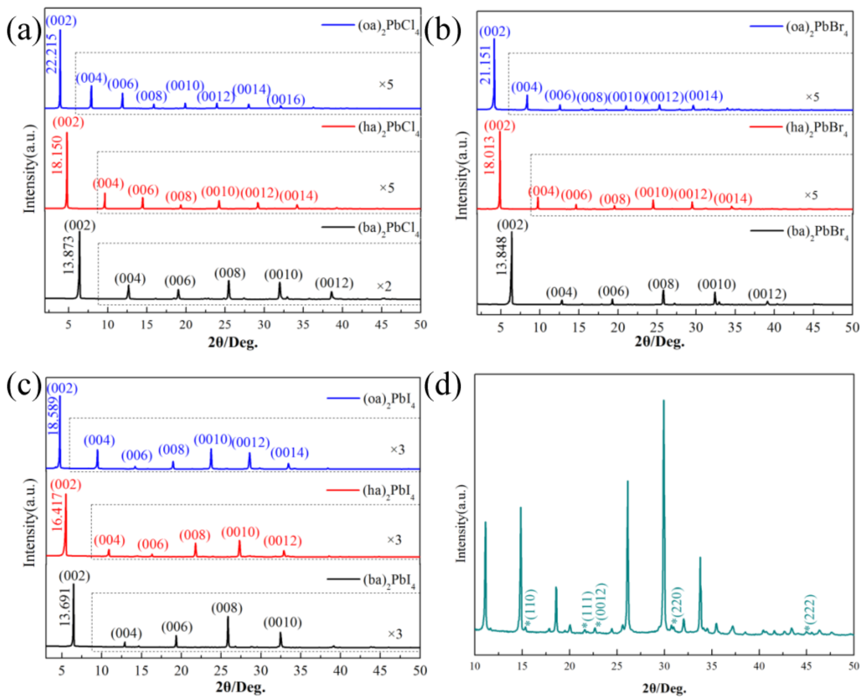

Figure S1. XRD patterns of (a-c) L_2PbX_4 (L = ba, ha, oa; X = Cl, Br, I); (b) The local enlargement XRD pattern for $(ha)_2CsPb_2Br_7$ with the angles ranging from 10°~ 50°.

Table S1. The main XRD peak data of $(ha)_2CsPb_2Br_7$

2θ(deg.)	**(hkl)**	**d_{hkl}(Å)**
3.73	(002)	23.720
11.11	(006)	7.9608
14.84	(008)	5.8905
15.33	(110)	5.7781
18.58	(0010)	4.7759
21.59	(111)	4.0715
22.66	(0012)	3.9236
26.12	(0014)	3.4113
29.93	(0016)	2.9450
30.97	(220)	2.8678
33.78	(0018)	2.6532
44.87	(222)	2.0255

Table S2. Elemental analysis and ICP for $L_2Cs_{n-1}Pb_nX_{3n+1}$(L = ba, ha, oa; X = Cl, Br, I; *n* = 1, 2)

Perovskites		**C (wt%)**	**H (wt%)**	**N (wt%)**	**Pb (μg/mL)**
$(ba)_2PbCl_4$	Calculated value	19.40	4.48	5.66	39.82
	Elemental analysis	19.03	4.16	5.21	38.54
$(ha)_2PbCl_4$	Calculated value	26.14	5.48	5.08	69.14
	Elemental analysis	25.7	5.287	4.97	69.44
$(oa)_2PbCl_4$	Calculated value	31.633	6.305	4.611	40.929
	Elemental analysis	31.37	6.344	4.57	42.04
$(ba)_2PbBr_4$	Calculated value	14.28	3.294	4.16	38.171
	Elemental analysis	14.21	3.297	4.15	38.13
$(ha)_2PbBr_4$	Calculated value	19.77	4.15	3.84	46.60
	Elemental analysis	19.61	4.36	3.83	44.71
$(oa)_2PbBr_4$	Calculated value	24.471	4.877	3.567	22.163
	Elemental analysis	25.00	5.211	3.66	21.6
$(ba)_2PbI_4$	Calculated value	11.159	2.575	3.253	39.46
	Elemental analysis	10.73	2.646	3.11	38.92
$(ha)_2PbI_4$	Calculated value	15.714	3.297	3.054	57.83
	Elemental analysis	15.98	3.423	3.13	56.57
$(oa)_2PbI_4$	Calculated value	19.744	3.935	2.878	33.21
	Elemental analysis	18.89	4.045	2.78	31.53
$(ha)_2 CsPb_2Br_7$	Calculated value	11.01	2.31	2.14	51.918
	Elemental analysis	11.12	2.425	2.15	50.48

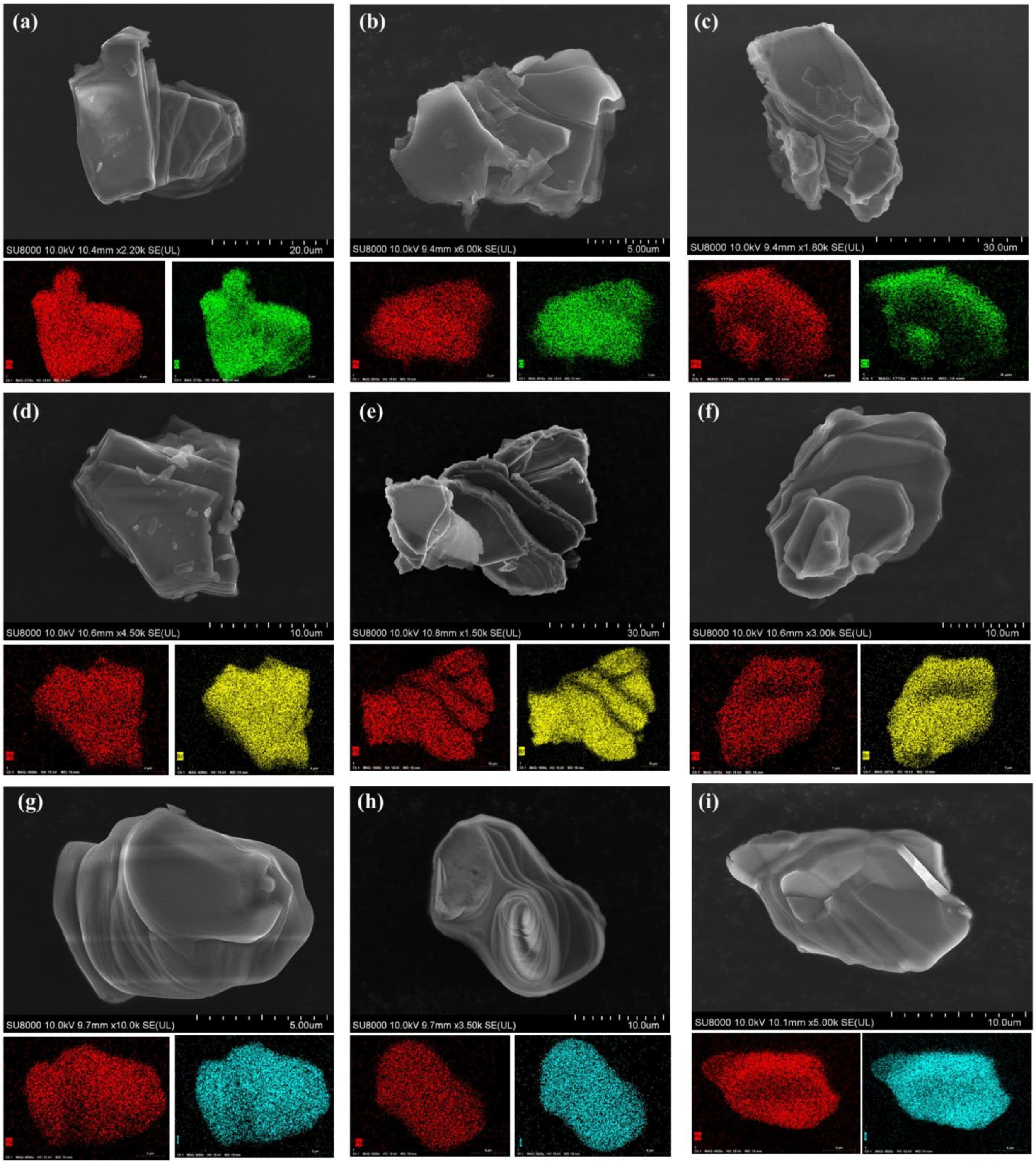

Figure S2. SEM and EDS images of (a) $(ba)_2PbCl_4$, (b) $(ha)_2PbCl_4$, (c) $(oa)_2PbCl_4$, (d) $(ba)_2PbBr_4$, (e) $(ha)_2PbBr_4$, (h) $(oa)_2PbBr_4$, (g) $(ba)_2PbI_4$, (h) $(ha)_2PbI_4$ and (i) $(oa)_2PbI_4$. Corresponding element mapping in SEM image Pb (red), Cl (green), Br (yellow) and I (blue).

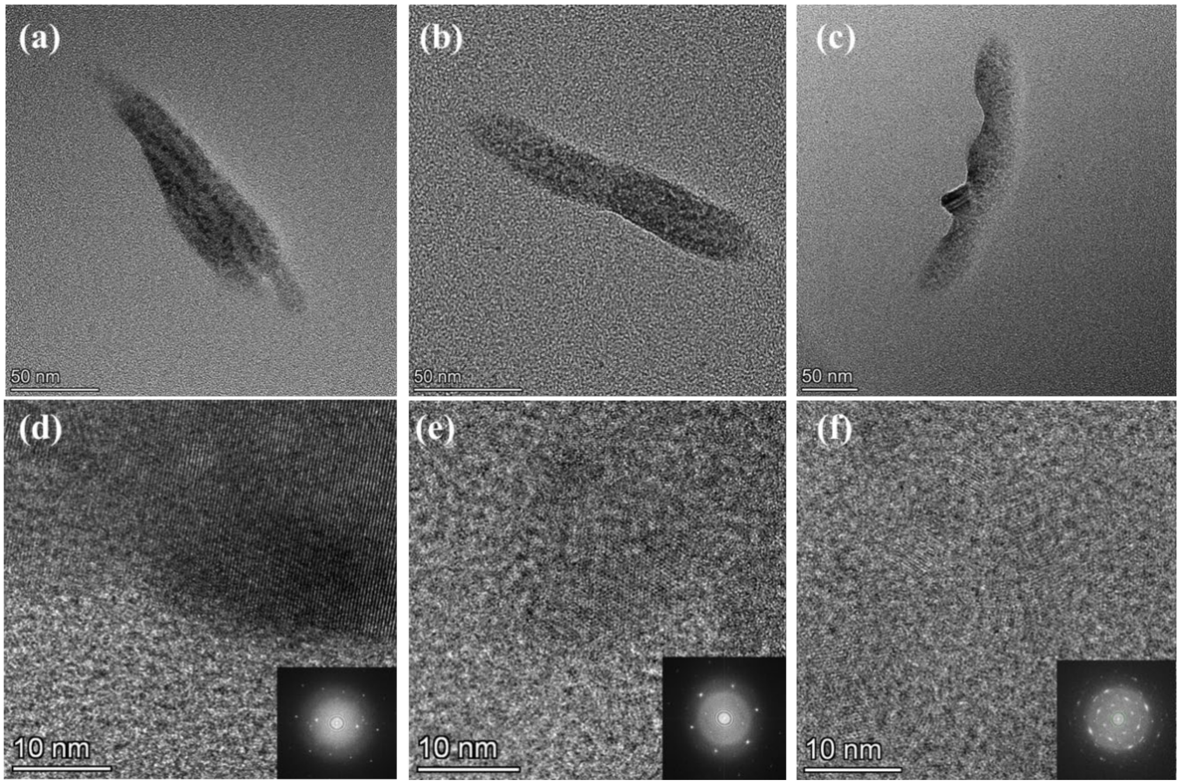

Figure S3. TEM images(a-c) , HRTEM images(d-f) (the right bottom panel is FFT pattern) of (a) $(ha)_2PbCl_4$, (b) $(ha)_2PbBr_4$ and (c) $(ha)_2PbI_4$.

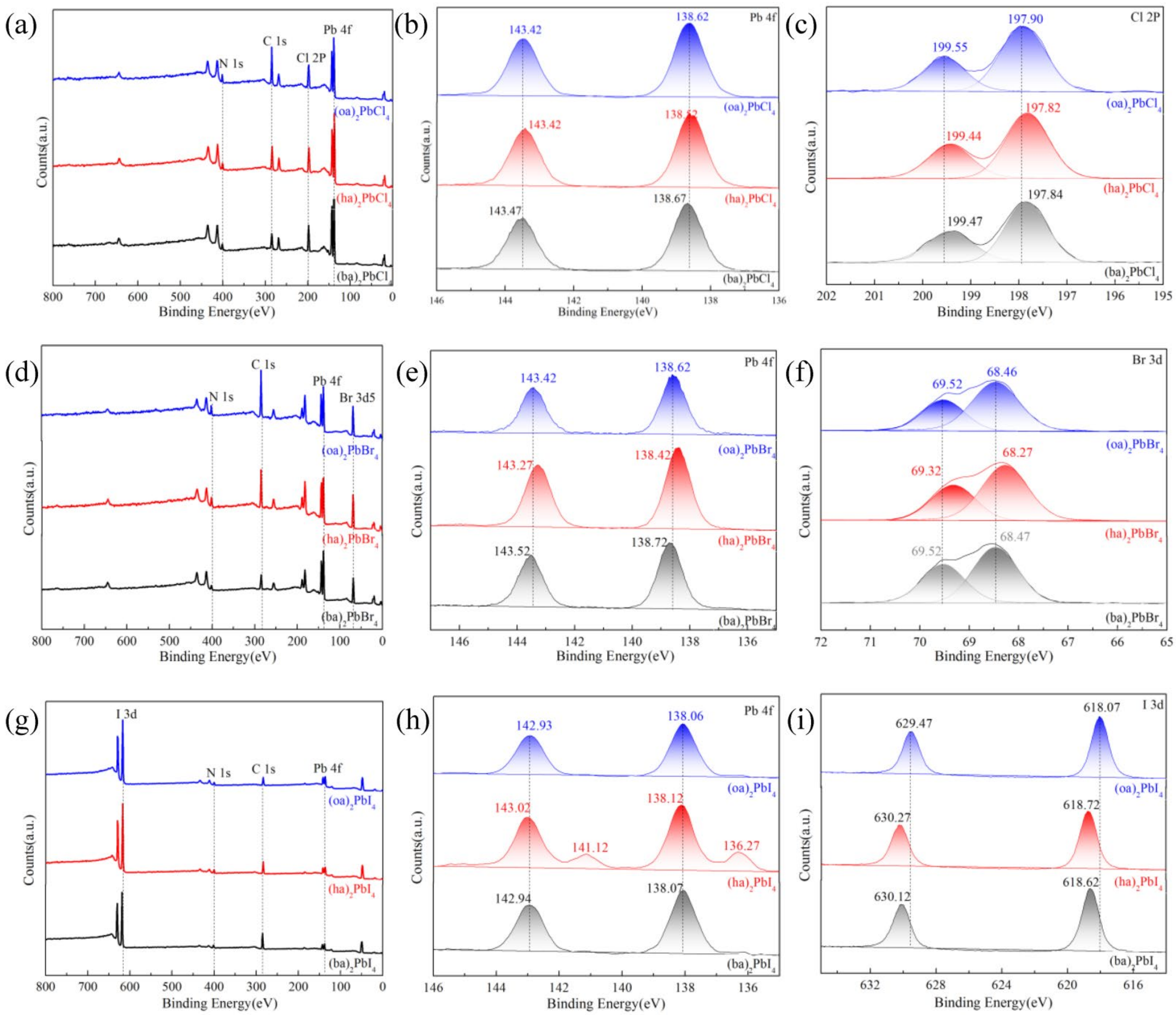

Figure S4. XPS spectra corresponding to (a,d,g) survey, (b,e,h) Pb 4f, (c)Cl 2P, (f)Br 3d and (i)I 3d of L_2PbCl_4(a-c), L_2PbBr_4(d-f) and L_2PbI_4(g-i)(L = ba, ha, oa). The binding energy is calibrated with the C 1s peak (284.5 eV) of free carbon.

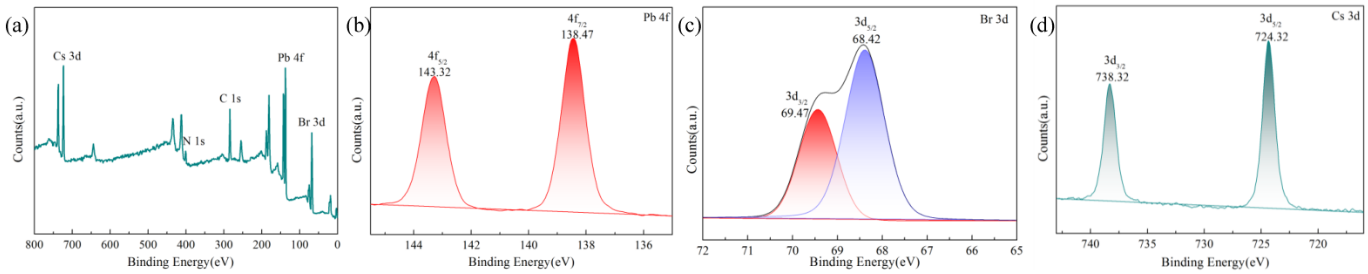

Figure S5. XPS spectra of $(ha)_2CsPb_2Br_7$ (a)survey, (b)Pb 4f, (c)Br 3d and (d)Cs 3d. The binding energy is calibrated with the C 1s peak (284.5 eV) of free carbon.

Table S3. Quantitative XPS analysis of $L_2Cs_{n-1}Pb_nX_{3n+1}$(L = ba, ha, oa; X = Cl, Br, I; n = 1, 2).

Perovskites	Atomic Ratio (%)		
	Pb	**X**	**Cs**
$(ba)_2PbCl_4$	10.18	38.55	
$(ha)_2PbCl_4$	8.18	31.6	
$(oa)_2PbCl_4$	5.22	20.96	
$(ba)_2PbBr_4$	8.33	31.45	
$(ha)_2PbBr_4$	4.11	17.15	/
$(oa)_2PbBr_4$	3.51	16.21	
$(ba)_2PbI_4$	4.47	18.71	
$(ha)_2PbI_4$	2.48	12.18	
$(oa)_2PbI_4$	1.56	6.86	
$(ha)_2$ $CsPb_2Br_7$	6.34	24.93	3.47

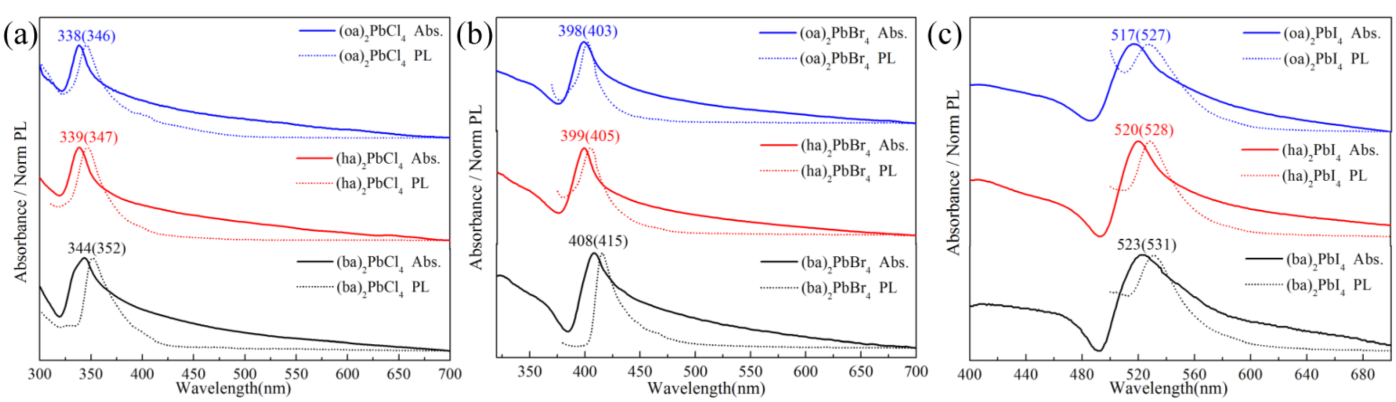

Figure S6. UV−vis absorption(solid line) and PL emission spectra(dotted line) of (a)L_2PbCl_4, (b) L_2PbBr_4, (c) L_2PbI_4(L = ba, ha, oa)

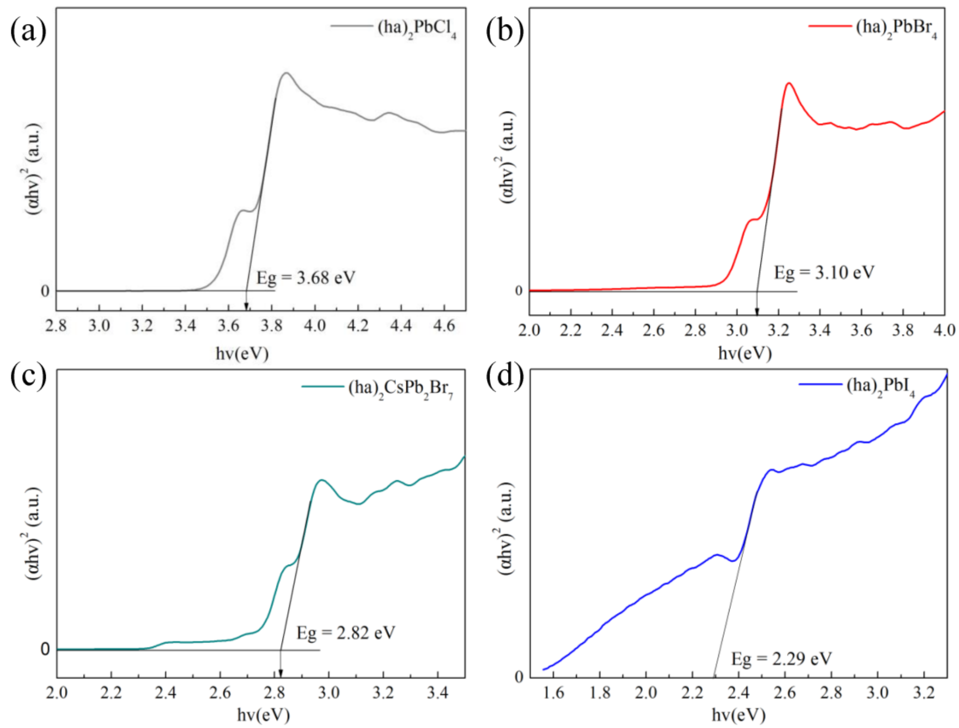

Figure S7. Tauc plots of (a)$(ha)_2PbCl_4$ (b) $(ha)_2PbBr_4$ (c) $(ha)_2CsPb_2Br_7$ (d) $(ha)_2PbI_4$

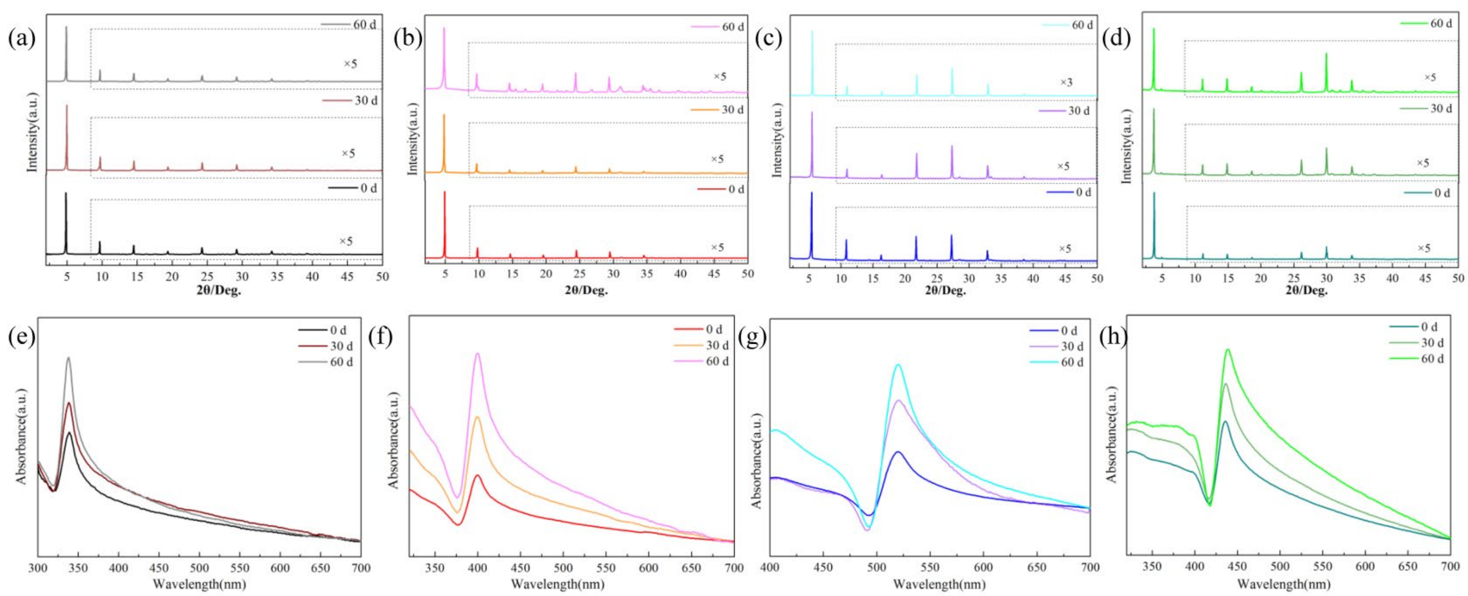

Figure S8. XRD patterns of (a)$(ha)_2PbCl_4$ (b) $(ha)_2PbBr_4$ (c) $(ha)_2PbI_4$ (d) $(ha)_2CsPb_2Br_7$ and corresponding to UV−vis absorption spectra(e-h) after several days under atmosphere environment.

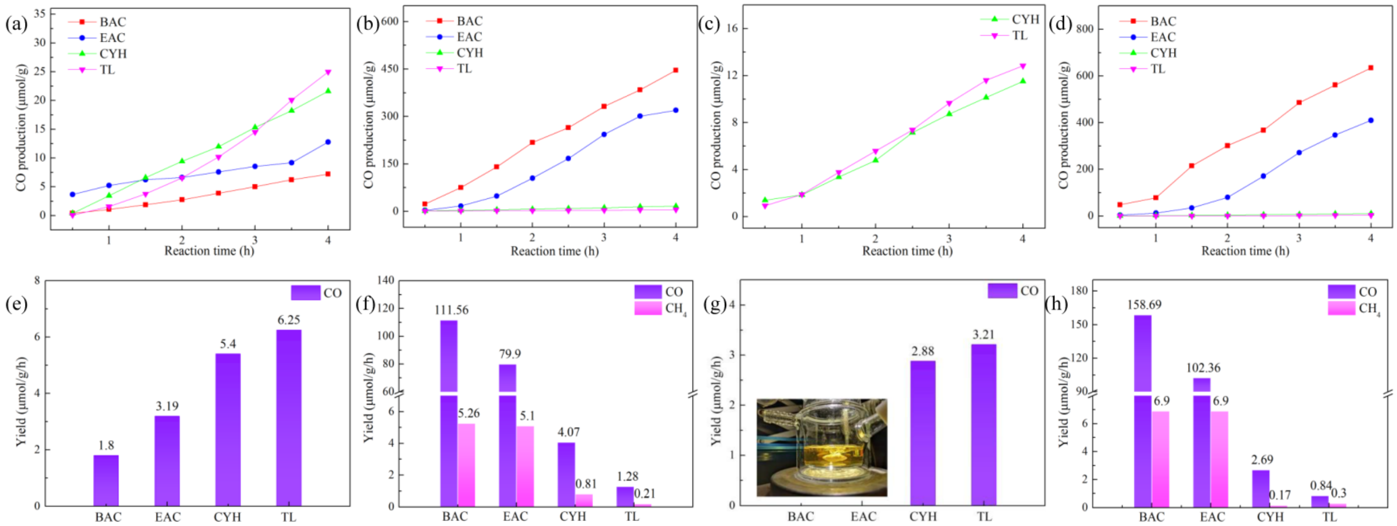

Figure S9. Photocatalytic evolution of CO for photocatalytic catalyst in various solvents (300 W Xe lamp, with the light intensity of 400 mW and the light source of full wavelength). (a)$(ha)_2PbCl_4$ (b) $(ha)_2PbBr_4$ (c) $(ha)_2PbI_4$ (d) $(ha)_2CsPb_2Br_7$ and corresponding to CO and CH_4 yield after 4 h of photochemical reaction(e-h).

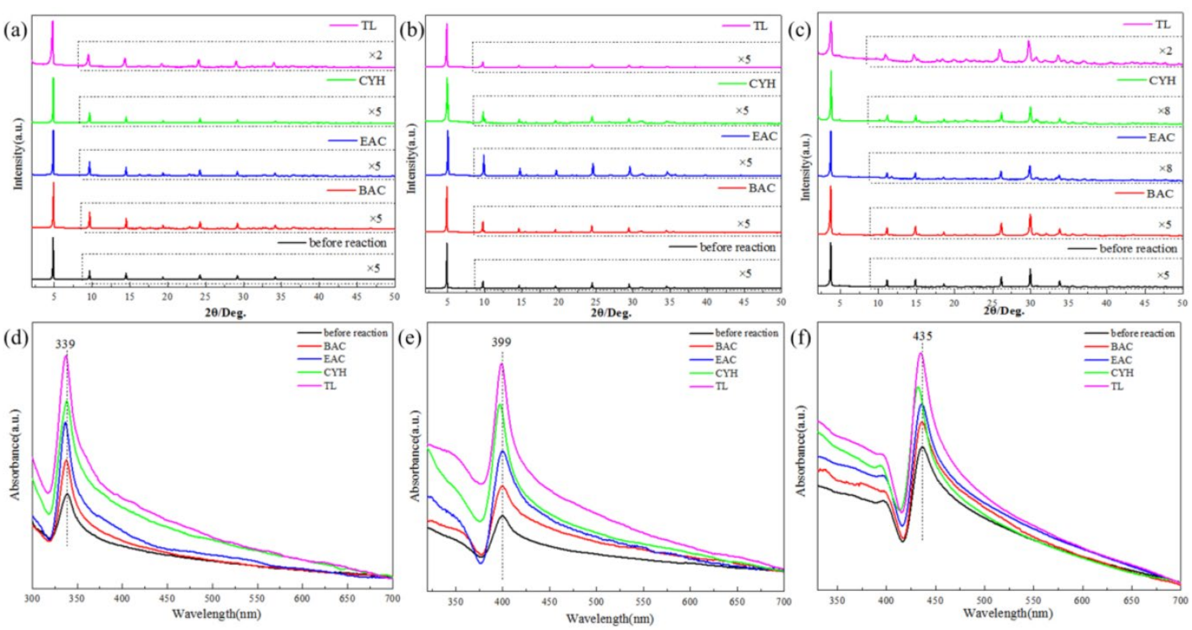

Figure S10. XRD patterns of (a)$(ha)_2PbCl_4$ (b) $(ha)_2PbBr_4$ (c) $(ha)_2CsPb_2Br_7$ in various solvents and corresponding to UV−vis absorption spectra(d-f) after 4 h of photochemical reaction (300 W Xe lamp, with the light intensity of 400 mW and the light source of full wavelength).

Table S4. Summary of reported photocatalytic CO_2 reduction performance.(Most of them are perovskite-based photocatalysts)

Photocatalyst	**conditions**	**Light source/Intensity**	**Products /μmol·g⁻¹·h⁻¹**	**Ref.**
$(ha)_2CsPb_2Br_7$	butyl acetate	300W Xe lamp 400 mW	CO, 158.69 CH_4, 6.9	This work
Pt-$CsPbBr_3$/Bi_2WO_6	ethyl acetate /isopropanol	150W Xe Lamp AM 1.5G 150 mW/cm^{-2}	CO, 17.2 CH_4, 34.4 H_2, 7.4	S1
$CsPbBr_3$/Cs_4PbBr_6	acetonitrile/ water/ methanol	300W Xe Lamp 100 mW/cm^{-2}	CO, 45.2	S2
$Co_{1\%}$@ $CsPbBr_3$/Cs_4PbBr_6			CO, 122.33	
$CsPbBr_3$	ethyl acetate/water and acetonitrile/water	300W Xe lamp ＞420 nm	CO, ＜10 CH_4, ＜10	S3
$CsPbBr_3$/g-C_3N_4	acetonitrile/water		CO, 148.9	
	ethyl acetate/water		CO, ＜70	
Mn/CsPb(Br/Cl)$_3$	ethyl acetate	300W Xe Lamp AM 1.5G	CO, 213 CH_4, 9.1	S4
$CsPbBr_3$-Glycine	gas (CO_2+H_2O)	300W Xe lamp 100 mW/cm^{-2}	CO, 27.7	S5
$CsPbBr_3$	ethyl acetate	300W Xe Lamp AM 1.5G	CO, 15 CH_4, 6.7	S6
$CsPb(Br_{0.5}/Cl_{0.5})_3$			CO, 85.2 CH_4, 12	
$CsPbBr_3$/g-C_3N_4	deionized water	300W Xe Lamp	CO, 6.1	S7
$CsPbBr_3$/g-C_3N_4	toluene	300W Xe lamp ＞420 nm	CO, 28.5	S8
$CsPbBr_3$	gas (CO_2+H_2O)	300W Xe lamp 100 mW/cm^{-2}	CO, 21.6	S9
$CsPbBr_3$	acetonitrile/water	300W Xe lamp ＞420 nm 150 mW/cm^{-2}	CO, 7.78 CH_4, 3.93	S10
C_{60}/$CsPbBr_3$			CO, 17.83 CH_4, 6.83	
$Cs_4Pb_3Br_{10}$ (n = 3); $Cs_5Pb_4Br_{13}$ (n = 4)	gas (CO_2+H_2O)	300W Xe lamp AM 1.5G 100 mW/cm^{-2}	CO, 25.96; 38.27 CH_4, 2.67; 2.88	S11
$Cs_4Pb_3Br_{10}$/RGO; $Cs_5Pb_4Br_{13}$/RGO			CO, 54.82; 81.39 CH_4, 4.20; 3.86	
$Cs_3Sb_2(Br_{0.7}I_{0.3})_9$	gas (CO_2+H_2O)	300W Xe lamp ＞420 nm	CO, 27.7	S12
$Cs_3Bi_2Br_9$	isopropanol	300W Xe lamp 200-1100 nm 70 mW/cm^{-2}	CO, 8.58 CH_4, 5.36	S13
$Cs_2AgBiBr_6$			CO, 7.34 CH_4, 0.75	
$ZnFe_2O_4$/Ag/TiO_2	H_2O	200 Hg lamp 150mW cm^{-2}	CO, 1025 CH_4, 132 CH_3OH, 31	S14
CuNi/C	TEOA-H_2O	300 W Xe lamp	CO, 11.205 CH_4, 0.9	S15

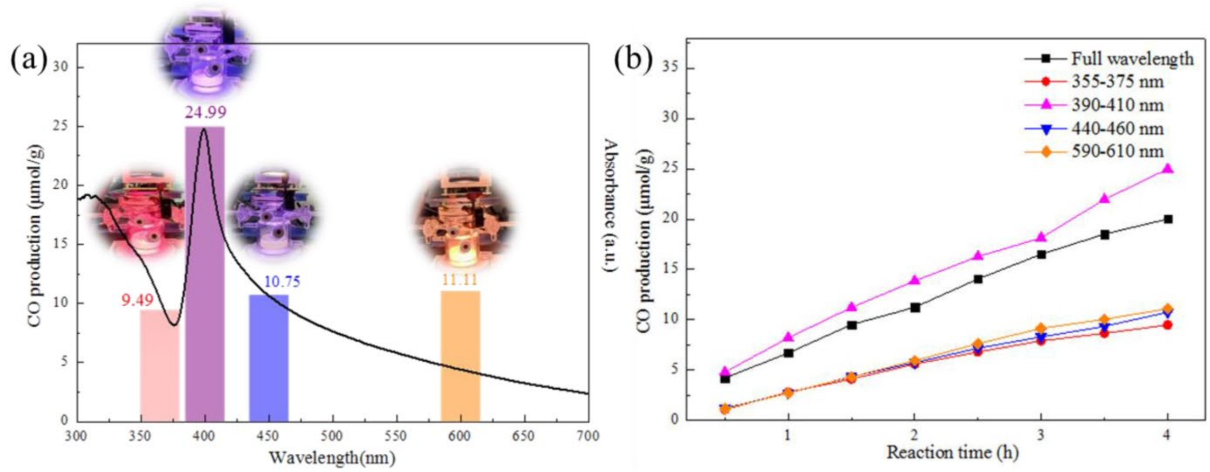

Figure S11. (a) UV-vis absorption spectrum of $(ha)_2PbBr_4$ and CO yield under monochromic sources after 4 h of photocatalytic reaction (the illustration show the corresponding monochromic light sources); (b) Photocatalytic evolution of CO under monochromic light sources (300 W Xe lamp, with the light intensity of 50 mW).

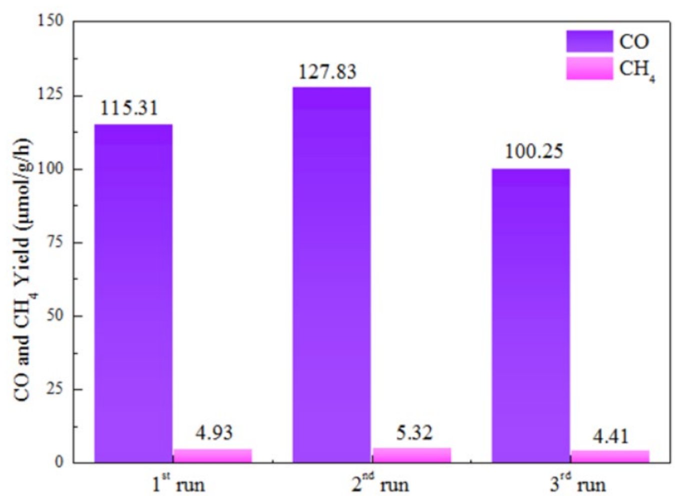

Figure S12. CO and CH_4 yield of $(ha)_2CsPb_2Br_7$ as photocatalyst and BAC as solvent for three consecutive runs of 4 h each time (300 W Xe lamp, with the light intensity of 400 mW and the light source of full wavelength).

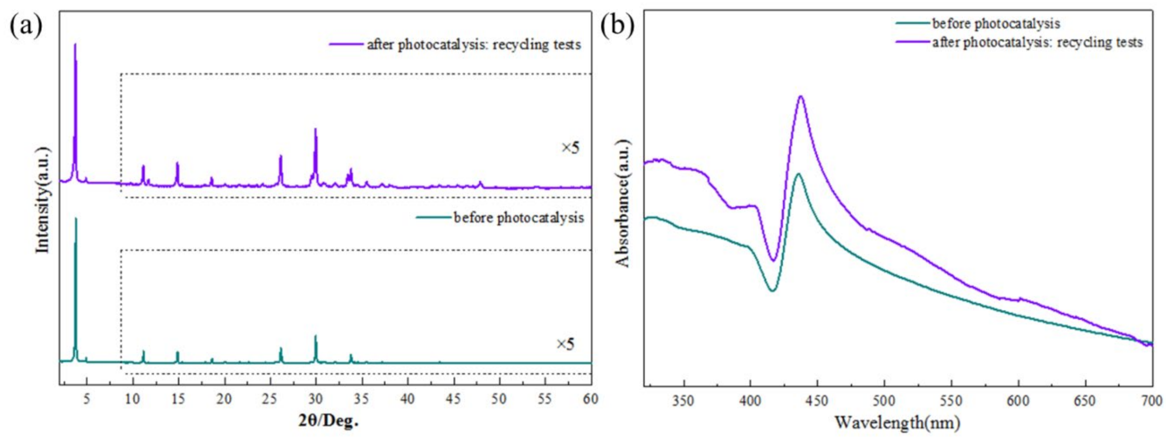

Figure S13. (a) XRD patterns and (b) UV-vis spectra of $(ha)_2CsPb_2Br_7$ after photocatalytic reaction (300 W Xe lamp, with the light intensity of 400 mW and the light source of full wavelength).

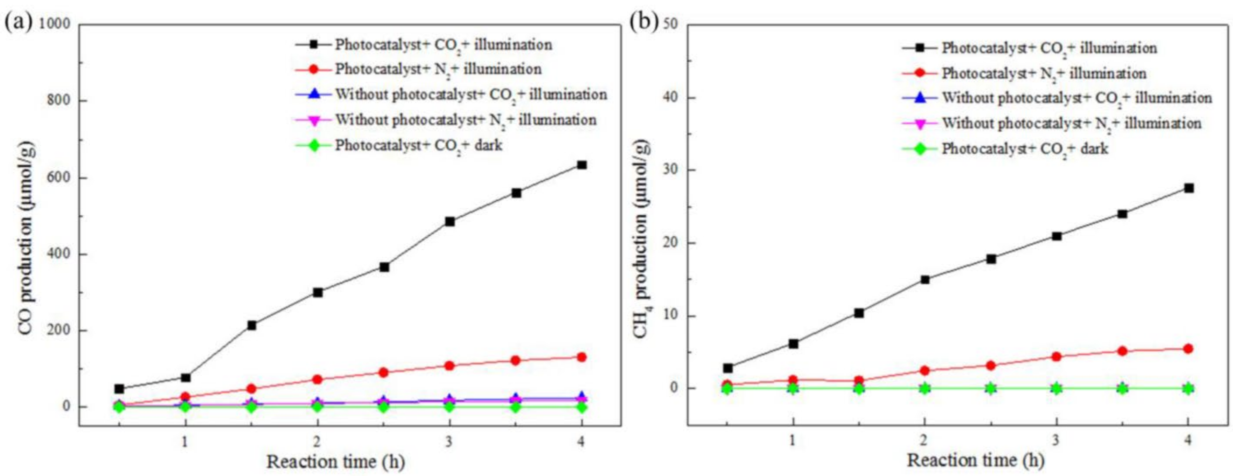

Figure S14. Photocatalytic evolution of products in different conditions with $(ha)_2CsPb_2Br_7$ as photocatalyst and BAC as solvent (300 W Xe lamp, with the light intensity of 400 mW and the light source of full wavelength). (a)CO and (b)CH_4.

REFERENCES

S1 Y. Jiang, H. Y. Chen, J. Y. Li, J. F. Liao, H. H. Zhang, X. D. Wang and D. B. Kuang, *Adv. Funct. Mater.*, 2020, **30**, 2004293.

S2 G. Dong, W. Zhang, Y. Mu, K. Su, M. Zhang and T. Lu, *Chem. Commun.*, 2020, **56**, 4664.

S3 M. Ou, W. G. Tu, S. M. Yin, W. N. Xing, S. Y. Wu, H. J. Wang, S. P. Wan, Q. Zhong and R. Xu, *Angew. Chem. Int. Ed.*, 2018, **57**, 13570.

S4 Y. Liu, S. Guo, S. You, C. Sun, X. Wang, L. Zhao and Z. Su, *Nanotechnology*, 2020, **31**, 215605.

S5 Y. Xu, W. Zhang, K. Su, Y. X. Feng, Y. F. Mu, M. Zhang and T. B. Lu, *Chem. Eur. J.*, 2021, **27**, 2305.

S6 S. Guo, J. Zhou, X. Zhao, C. Sun, S. You, X. Wang and Z. Su, *J. Catal.*, 2019, **369**, 201.

S7 Y. Wang, Z. Liu, X. Tang, P. Huo, Z. Zhu, B. Yang and Z. Liu, *New J. Chem.*, 2021, **45**, 1082.

S8 R. Cheng, H. Jin, M. B. J. Roeffaers, J. Hofkens and E. Debroye, *ACS Omega*, 2020, **5**, 24495.

S9 L. Wu, M. Zhang, Y. Feng, W. Zhang, M. Zhang and T. Lu, *Solar RRL*, 2021, **5**, 2100263.

S10 Z. Zhang, M. Shu, Y. Jiang and J. Xu, *Chem. Eng. J.*, 2021, **414**, 128889.

S11 C. C. Lin, J. Y. Li, N. Z. She, S. K. Huang, C. Y. Huang, I. T. Wang, F. L. Tsai, C. Y. Wei, T. Y. Lee, D. Y. Wang, C. Y. Wen, S. S. Li, A. Yabushita, C. W. Luo, C. C. Chen and C. W. Chen, *Small*, 2022, 2107881.

S12 D. F. Wu, B. J. Huo, Y. Y. Huang, X. S. Zhao, J. Y. Yang, K. Hu, X. C. Mao, P. He, Q. Huang and X. S. Tang, *Small*, 2022, **18**, 2106001.

S13 Q. M. Sun, J. J. Xu, F. F. Tao, W. Ye, C. Zhou, J. H. He and J. M. Lu, *Angew. Chem. Int. Ed.*, 2022, e202200872.

S14 Muhammad Tahir, *J. CO_2 Util.*, 2020, **37**, 134.

S15 H. Jiang, S. Q. Gong, S. Xu, P. H. Shi, J. C. Fan, V. Cecen, Q. J. Xu, and Y. L. Min, *Dalton Trans.*, 2020, **49**, 5074.